Simulation of earthquake-induced structural vibrations in systems with SMA damping elements*

Stefan Seelecke[1], Olaf Heintze[2], Arata Masuda[3]
[1]North Carolina State University, Center for Research in Scientific Computation
[2]North Carolina State University, Department of Mechanical & Aerospace Engineering
[3]Kyoto Institute of Technology, Department of Mechanical and System Engineering
email: stefan_seelecke@ncsu.edu (corresponding author)

ABSTRACT

The paper studies the influence of a shape memory alloy (SMA) element on the dynamic response of a single-degree-of-freedom-system, representing a structural building under earthquake excitation. Variations of the SMA geometry are studied by numerical simulation, and a value for the SMA radius is determined, which provides optimal system performance. In particular do we focus on the role of hysteresis-induced passive damping, which can potentially be exploited for the development of SMA-based semi-active control schemes.

1 Introduction

Over the past several decades, significant efforts have focused on mitigation of earthquake disasters by improving the structural safety and thereby reducing the loss in life and economy. Recent advances in new materials and technologies including sensing, non-destructive evaluation, system identification, and response control methodologies (e.g., Housner et al.,[1] Liu et al.[2,3] and Fujino et al.[4]) may be witnessed as part of such efforts. After having established themselves in engineering disciplines like mechanical and aerospace engineering, so-called smart materials have become increasingly popular in the civil engineering field as well. This is in particular related to the possibility of controlling structural vibrations in an effective way. Major research and development efforts in recent years have lead to efficient control systems making use of electro- or magnetorheological dampers, see Spencer and Sain[5] for an overview of the subject.

Another representative of the smart materials class which can be of interest for structural damping applications, are shape memory alloys (SMAs). After having been introduced as actuators in adaptive structures and mechatronics solutions, they have started to attract increasing attention due to their dynamic properties. The hysteretic phase transformation between austenite and martensite at high temperature and between different twins of the martensite phase at low temperature constitutes an intrinsic dissipation mechanism, which results in a considerable damping capacity. Figure 1 shows a hysteresis loop typical for NiTi in the pseudoelastic high temperature regime. Graesser and Cozarelli[6] first suggested the use of SMAs as novel damping materials and Clark et al[7] demonstrated the feasibility of the concept for a Nitinol wire device. Potential applications are seen amongst others in civil structures like buildings and bridges where SMAs can provide an efficient seismic base isolation; see Wilde et al.[8] The subject has been quite extensively covered experimentally, and a very good overview can be found in the reports of the European MANSIDE project.[9]

*to appear in Proceedings of the SPIE Smart Structures & Materials 2002, Vol. 4697, San Diego, 2002

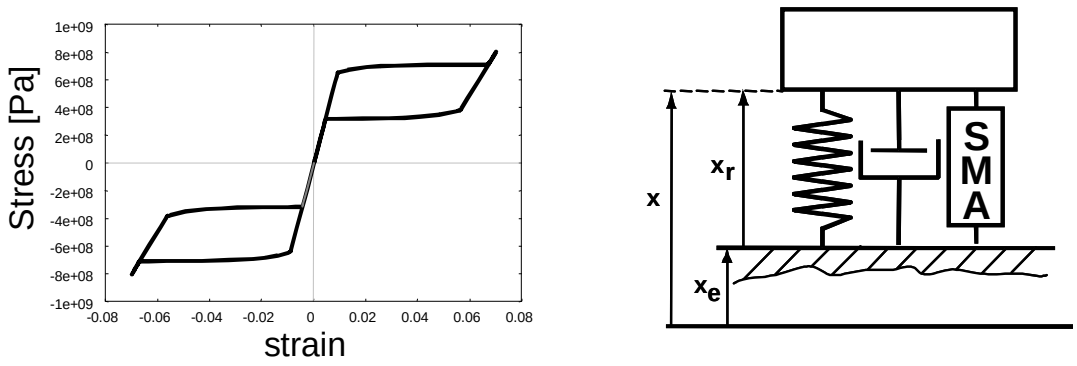

Figure 1: Typical pseudoelastic hysteresis loop in a NiTi shape memory alloy (left) and Single-Degree-of-Freedom system containing SMA element (right).

The present paper focuses on the the influence of geometry variations of a pseudoelastic SMA damping element on the dynamic response of a single degree of freedom (SDOF) system under a typical earthquake excitation. In particular are we interested to find the relation between the geometry and an optimal passive damping behavior. This will yield additional insight for design criteria as well as for the development of a semi-active control algorithm to be studied in a forthcoming paper.

A numerical simulation of the above system is performed to study the SMA-related damping behavior. After a short review of the basic model equations, we try to clarify the role of stiffness and damping, which is always simultaneously introduced into a system by adding a SMA element. We then study the role of the SMA radius and give a combined criterion to choose this radius in an optimal way.

2 Constitutive model and equations of motion

The SMA behavior is simulated using an improved version of the model originally suggested by Müller and Achenbach.[10,11] Even though this model is particularly suited for a dynamic application by reproducing strain-rate dependent self-heating and -cooling, we only use it here in an isothermal setting as a first step. This way, we can concentrate on the generic role of phase transformation and hysteresis, and illustrate the SMA-related damping contributions without additional complexity.

The SDOF system in Figure 1 is chosen such as to represent a 15-story-building with typical stiffness and damping values for its first bending mode. The building's excitation is given by acceleration data recorded from the east-west (EW) component of the Tafts 1952 earthquake, shown in Figure 2. To study the decay behavior of the vibration we doubled the length of the available recording, setting the acceleration to zero during the second half.

The equations of motion for such a case are most conveniently written in the relative coordinate system, which moves with the ground. They read

$$m\ddot{x}_r = -c\dot{x}_r - kx_r - F_{SMA} - m\ddot{x}_e\left(t\right) \quad , \tag{1}$$

where c is the damping coefficient, k the stiffness and $\ddot{x}_e\left(t\right)$ the excitation acceleration from Figure 2. F_{SMA} is the force exerted on the structure by a SMA element.

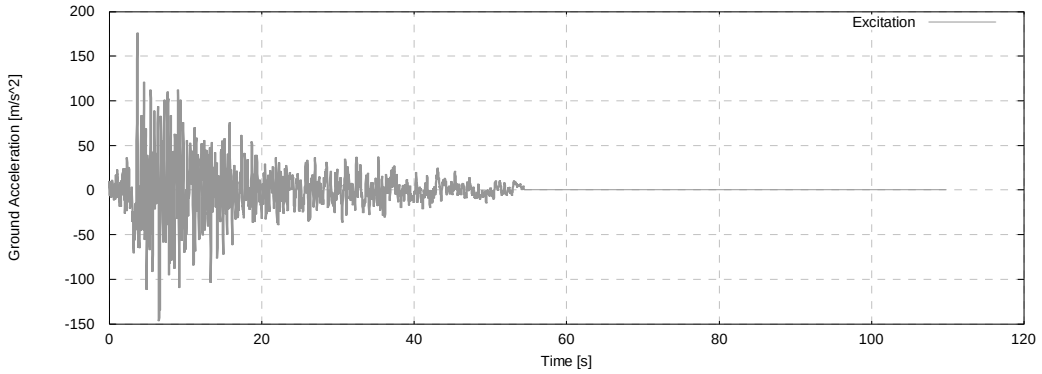

Figure 2: Ground acceleration from EW component of 1952 Tafts earthquake.

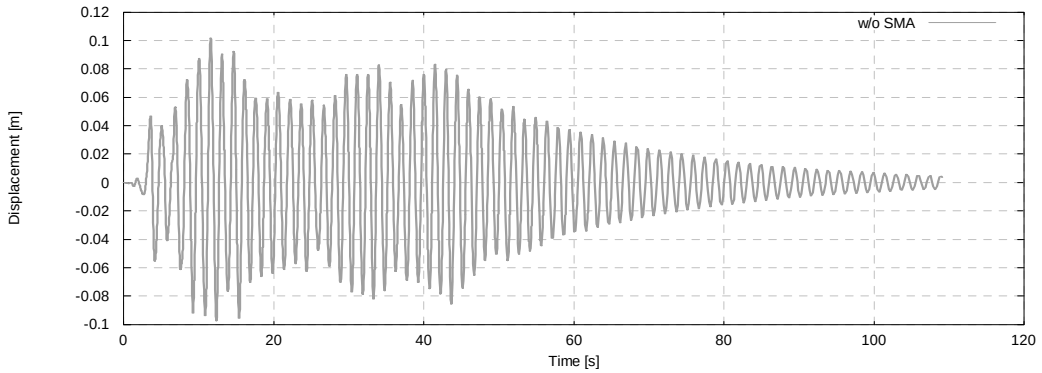

Figure 3: System response without SMA.

Figure 3 shows the displacement of the structure without a SMA element, and this response will serve as a reference to compare against for the cases with SMA element. The values chosen for mass, stiffness and damping are $m = 2.8e6\ kg$, $k/m = 17.55/s^2$ and $c/m = 0.084/s$.

Before we proceed to study the influence of a SMA element, we will give a short review of the SMA model equations, which are used to calculate the force F_{SMA}.

The model assumes one-dimensional behavior, in which case the SMA can exist in three possible phases, viz. austenite A or one of two martensitic twin phases, denoted by $M_{\pm}$. The macroscopic body is composed of layers stacked on top of each other, and each layer can be in either of the three phases. Due to the thermal activation present in every physical system, the layers fluctuate about their equilibrium strain values, and, depending on stress and temperature, they can undergo a transformation from one phase into another. The average strain in such a material is given by the weighted sum of the average strains in the individual phases, ε_A and $\varepsilon_{\pm}$, and reads

$$\varepsilon = x_+ \varepsilon_+ (\sigma) + x_- \varepsilon_- (\sigma) + x_A \varepsilon_A (\sigma) . \tag{2}$$

The central constitutive quantity is the stress and temperature dependent free energy; and with its knowledge we can calculate the average strains as functions of stress using methods from statistical thermodynamics.

The weighting factors in (2) are the phase fractions x_A and $x_{\pm}$, and they follow from a set of evolution

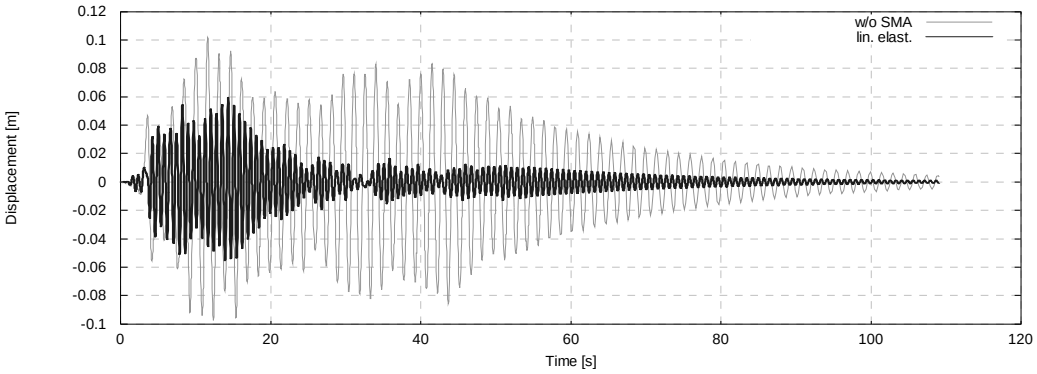

Figure 4: System response with a non-transforming SMA.

equations motivated by the theory of thermally activated processes,

$$\dot{x}_+ = -x_+ p^{+A} + x_A p^{A+} \text{ and} \tag{3a}$$

$$\dot{x}_- = -x_- p^{-A} + x_A p^{A-} \ . \tag{3b}$$

The quantities $p^{\alpha\beta}, \alpha \in \{A, +, -\}$, are the transition probabilities to transform from phase α to β, and they again follow from the Gibbs free energy of a SMA element G, e.g.,

$$p^{+A} = \frac{1}{\tau_x} \frac{\exp - \left(\frac{G(\varepsilon_B, T; \sigma)}{kT} \right)}{\int_{\varepsilon_B}^{\infty} \left(\frac{G(\varepsilon, T; \sigma)}{kT} \right) d\varepsilon} \ . \tag{4}$$

In (4), T is the temperature, k is Boltzmann's constant, τ_x is a typical relaxation time for the phase transformation, and ε_B are typical strain values, which separate one phase from another. For a more detailed derivation of the model, see, e.g., Seelecke.[12]

Inverting Equation (2), we obtain the stress at each point in time from the strain ε, which is simply x_r/L_0, where L_0 is the initial length of the SMA. This stress, multiplied by the cross sectional area of the SMA, provides the force F_{SMA} on the RHS of Equation (1), which is necessary to solve the equations of motion.

3 Results

Before we turn to the variations in geometry, we first study the contribution of the individual effects caused by a SMA. In particular are we interested in illustrating the coupled effects of stiffness and damping naturally entering when adding a SMA element to a structure. A major advantage of a simulation is that we can easily separate these effects and thus study their individual contributions. Basically, there are three relevant mechanisms in a shape memory alloy, which is added to a structure performing a dynamic motion.

Firstly, it increases the stiffness of the system like an additional linearly elastic material. Secondly, beyond a certain stress threshold, it undergoes a phase transformation, which considerably softens the material and thirdly, this phase transformation is strongly hysteretic, thus dissipating a large amount of energy.

We start with comparing a system including a SMA, which does not undergo a phase transformation to

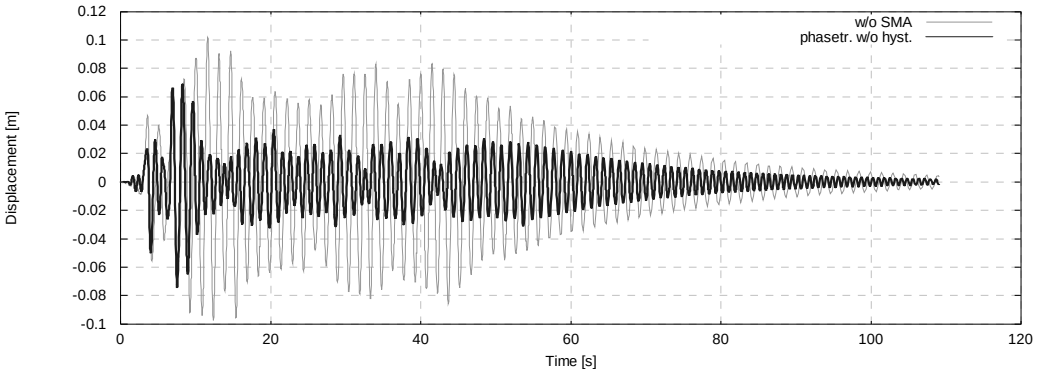

Figure 5: System response with non-hysteretic phase transformation in SMA element.

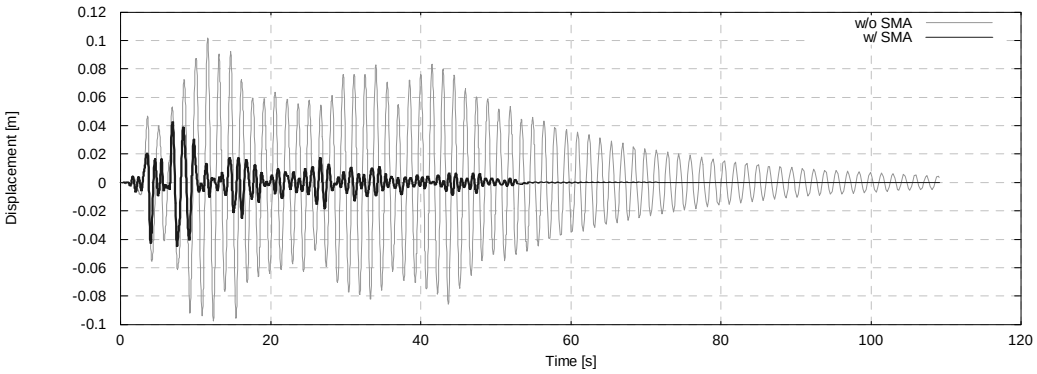

Figure 6: System response with hysteresis-induced damping by SMA.

the system without SMA. In this case, the SMA is modeled to remain completely austenitic during the entire vibration process. By inspection of Figure 4, it can be observed that the displacement amplitude has been considerably decreased. The price, however, is an increase in eigenfrequency, which has nearly doubled, leading to an undesirable increase in acceleration.

Figure 5, the case of hysteresis-free phase transformation, not surprisingly shows a substantial decrease in frequency over the non-transforming case(about 1.3 times the original frequency). On the other hand, it is by far not as efficient with respect to suppressing the system displacement, both of which effects have to be attributed to the lower equivalent stiffness of this case.

Figure 6 finally shows the results for the realistic SMA behavior, including the hysteresis-induced damping, and it becomes clear that this latter mechanism is the dominant effect for vibration reduction, also nearly preserving the original system's eigenfrequency.

All of the above calculations have been perfomed with a SMA length of $L_0 = 1m$ and a radius of $R = 0.025m$. The temperature was kept constant at $313K$.

From Figures 7 and 8 it becomes evident that for the above fixed value of L_0, the choice of R represents an optimum, at least for the case at hand. In order to characterize the system performance quantitatively we introduce a mean displacement and a mean acceleration, both measured in the relative system.

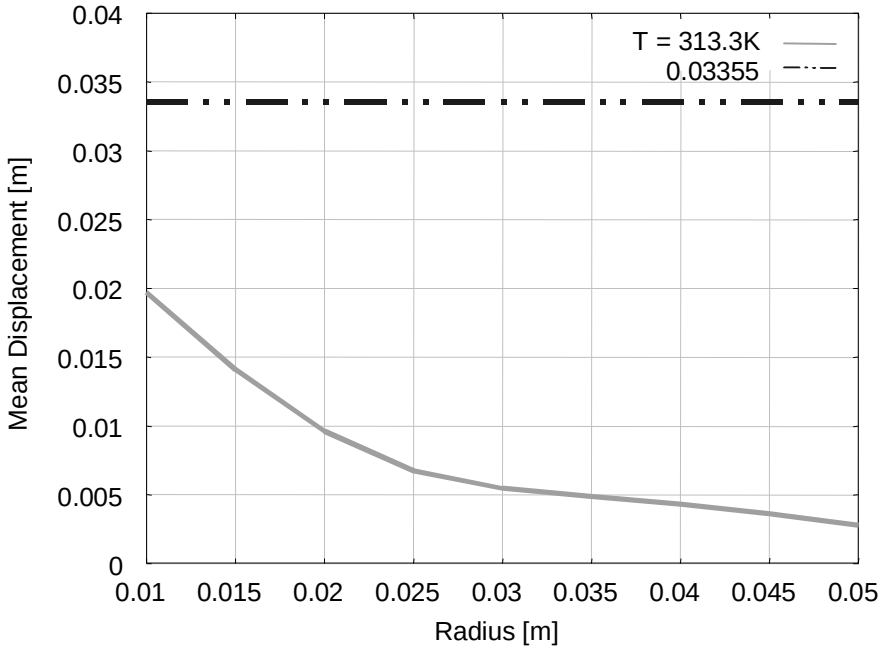

Figure 7: Mean system displacement as a function of SMA radius.

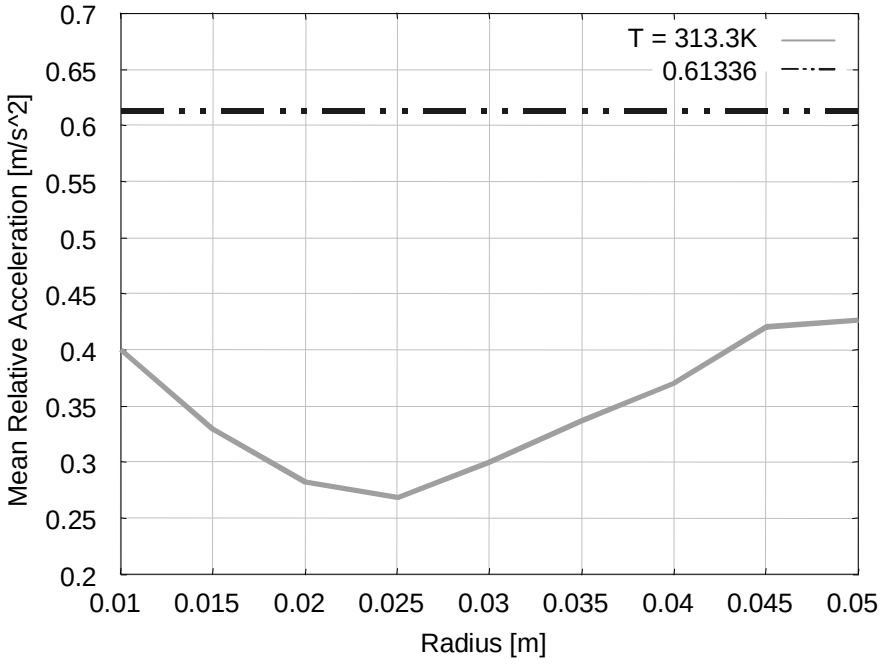

Figure 8: Mean relative system acceleration as a function of SMA radius.

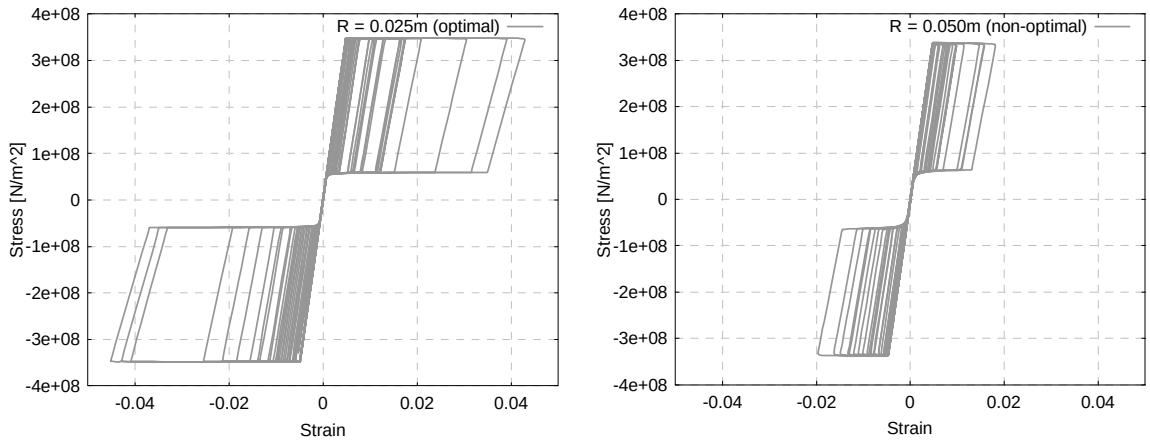

Figure 9: Dynamic hysteresis loops for the optimal (left) and non-optimal (right) radius, illustrating the different energy dissipation during the vibration processes.

They are defined as

$$\bar{x}_r = \sqrt{\frac{1}{T}\int_0^T x_r^2(t)\,dt} \quad \text{and}$$

$$\overline{\ddot{x}}_r = \sqrt{\frac{1}{T}\int_0^T \ddot{x}_r^2(t)\,dt} \quad \text{, respectively.}$$

While for increasing radius, the mean displacement decreases monotonously, see Figure 7, the mean acceleration in Figure 8 goes through a distinct minimum at $R = 0.025m$, before it starts to increase again. As a reference, the values of the system without SMA are plotted as the dash-dotted lines in both figures.

With this value, the mean displacement can be reduced by almost a factor of 5, while the acceleration is decreased by more than a factor of 2. Figure 6 shows that this does not only hold for the average value, but that also the maximum displacement amplitude has been decreased to nearly 40% of its original value.

Already the study of Figures 4, 5 and 6 seems to suggest that the hysteresis in the SMA is the major mechanism contributing to the damping, but this is made even clearer by the hysteresis loops in Figure 9. Here, we have plotted the dynamic stress-strain curves of the SMA during the processes, and it can be seen that the optimal case of $R = 0.025m$ features a considerably larger hysteretic area than the case with $R = 0.050m$.

4 Conclusions

Based on an isothermal version of the Müller-Achenbach-Seelecke model, the influence of geometry variations of a SMA element is studied, providing stiffness and damping to a structural system that vibrates under the excitation of an earthquake.

It is shown that a particular choise for the SMA radius leads to an optimal performance with respect to displacement and acceleration reduction. This is due to an optimal exploitation of the SMA's passive damping capacity, related to the large hysteresis in the material's stress-strain behavior.

The latter observation can be related to the ideas about optimally shaping the hysteresis, expressed in Masuda and Noori[13]; and it is the basis for the development of a SMA-based semi-active control system, which will be discussed in a forthcoming paper.

The work of SS was in part supported through NSF grant DMI-0134464.

5 REFERENCES

[1] Housner, G.W. et al (1997), "Structural Control: Past, Present, and Future," J. Engrg. Mech., ASCE, September

[2] Liu, S.C., Logorio, H.J., and Chong, K.P. (1993), "Status of U.S. Research on Structural Control Systems," Earthquake Spectra, Vol. 7, 543-550.

[3] Liu, S.C., Chong, K.P., Singh, M.P., and Sabadell, (1994) "Intelligent Renewal of the Nation's Infrastructures: A Bold Approach for Research and Development," Proc. of the First Conference on Structural Control, 3-5 August, Los Angeles

[4] Fujino, Y., Soong, T.T., Spencer, B.F., Jr, (1996), "Structural Control: Basic Concepts and Applications," Proc. ASCE Struct. Cong., XIV, Chicago, 1277-1287, April 1996

[5] Spencer B. F.; Sain, M. K. (1997) Controlling Buildings: A New Frontier in Feedback, Special Issue of the IEEE Control Systems Magazine on Emerging Technology, Vol. 17, No. 6, pp. 19-35

[6] Graesser, E.J., and Cozzarelli, F.A., (1991a). "Shape Memory Alloys as New Materials for Aseismic Isolation," J. Engrg Mech., ASCE, 117.11

[7] Clark, P.W., Aiken, I.D., Kelly, J.M., Higashino, and Krumme, R.C., (1995). Experimental and Analytical Studies of Shape Memory Alloy Dampers for Structural Control. Proc. 1995 Conf. on Smart Struct. and Mat

[8] Wilde K, Gardoni P and Fujino Y (2000), Base isolation system with shape memory alloy device for elevated highway bridges, Eng Struct, 22, 222-229.

[9] Memory Alloys for New Seismic Isolation and Energy Dissipation Devices (MANSIDE) (1999), Project Workshop Proceedings, published by The Italian Department of National Technical Services

[10] Achenbach M and Muller I (1985), Simulation of material behavior of alloys with shape memory, Arch Mech, 37, 573-585.

[11] Achenbach M (1989), A model for an alloy with shape memory, Int J Plast, 5, 371-395.

[12] Seelecke, S. (2002) "Modeling the Dynamic Behavior of Shape Memory Alloys", International Journal of Non-Linear Mechanics, Special Issue on Hysteresis and its Implications in Mechanics

[13] Masuda, A. and Noori, M. (2002) "Optimization of hysteretic characteristics of damping devices based on pseudoelastic shape memory alloys", International Journal of Non-Linear Mechanics, Special Issue on Hysteresis and its Implications in Mechanics